TECHNICAL REPORT

PART 1: DETAILED ELECTROMAGNETIC DESIGN OF AN INTEGRATED AND COMPACT 1.3 GHZ SUPERCONDUCTING RADIO FREQUENCY (SRF) ELECTRON SOURCE

N. Sipahi

Electrical and Computer Engineering Department, Colorado State University, Fort Collins, CO

Abstract

There exists a need for compact, reliable, high-power electron sources for applications including those in water treatment, basic science, defense, and security. There also exists a need for compact electron-beam based light and power sources of various power levels and at different frequencies (mm-wave to gamma rays) for applications also in the fields of basic science, industry, and defense and security. Today's examples of high-average-power electron sources are neither very compact nor highly efficient. The same may be said for many of the electron-beam based light sources operated worldwide for myriad of applications. Recent breakthroughs in superconducting (SC) materials technology, radio-frequency (RF) power systems, specialized cathodes, and RF cavity designs offer ways to overcome the above-mentioned shortcomings. In this report, all these new features are integrated in a comprehensive design into one promising concept for a compact superconducting RF (SRF) high-average power electron linear accelerator. This design is capable of 5-50 kW average electron beam power and continuous wave operation with the corresponding electron beam energy up to 10 MeV.

TABLE OF CONTENTS

LIST OF FIGURES

LIST OF TABLES

1. BACKGROUND AND GENERAL CONCEPT

A team from Fermilab, Colorado State University, Northern Illinois University, Euclid Techlabs, and PAVAC has started an effort to design, construct, and validate a compact, 10 kW average power linac capable of operating continuous wave (CW); delivering beam energies up to 10 MeV; weighing less than 3,000 pounds; and that can be palletized and made portable for a variety of industrial applications. This will be done by exploiting recent, robust, technological advancements in Superconducting Radio Frequency (SRF) and RF power source technologies as well as innovative solutions for the SRF gun and cathode system.

In this novel, envisioned design, the SRF system is inherently complex, but we have gathered a few recent enabling technologies and have included them in our overall system concept. These include the following.

- *A new Niobium processing technique* developed at Fermilab that allows us to achieve unprecedented Q_o (performance) values in superconducting RF cavities translating into very low losses and high efficiencies [1]. This opens up the possibility to operate such a cavity with cryo-coolers as the cooling requirements are only a few Watts. We can then do away with the costly and complex helium inventory and refrigeration system found on typical SRF systems.

- Fermilab has also developed *a new injection-locked magnetron RF source* and has tested this on a single, 2.45-GHz SRF cavity. The results show excellent amplitude and phase stability [2,3]. It has a very high efficiency (80%) and therefore a low cost per watt of operation. This RF source can be utilized to help

drive the overall cost of such an accelerator down to acceptable values. Furthermore, as the system architecture is standalone the cavity frequency is allowed to vary over time. As long as the RF system can track the frequency then the system continues to work. This greatly simplifies operation, as microphonics-induced frequency changes do not need to be corrected.

- Another innovation produced at Fermilab is the very *low heat leak fundamental power coupler* that would be used to input the primary RF power to the cavity [4]. Such a coupler should be able to sustain 10s of kW average power from the magnetron and waveguide into the SRF accelerator structure/cryomodule while nearly eliminating any heat load on the cooling system.

- Advances in understanding thermionic and field emission cathodes, in particular the potential to gate or limit their emission to acceptable phase values, invites the use of *a robust cathode system* in the SC environment. Indeed, this is one of the most significant challenges, but, in this report, we examine this challenge.

By combining the above technical advancements into the robust physics and engineering design described herein, a compact system similar to what is seen in Figure 1.1 can be realized [5].
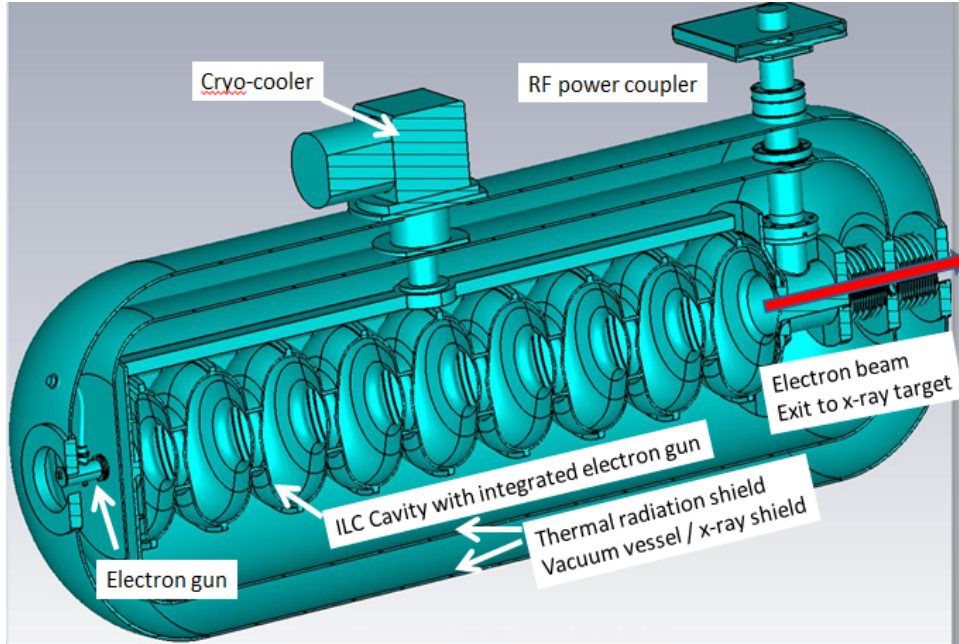
Figure 1: The concept for an integrated, compact, high-average power, SRF electron source. The overall length is roughly 1.5 m and the diameter is roughly 0.5 m. [5]

Such a compact system is certainly possible; however, there are many obstacles that still must be overcome to achieve such an integrated and functional design. This is the main idea of this study – to come up with an integrated system architecture of a compact, high-power electron source and then focus on the difficult issues to find workable solutions.

Our concentration has been on devising the cathode region design based on physical and engineering principles, coupling this design into an RF cavity acceleration structure, and building a parameterized model of this system. We have integrated the cathode, electron gun, and main accelerator into one fully integrated component as well as ensured that proper gating of that cathode limits any beam loss through the system that would have the deleterious effects described above. In this integration step, the design

of the cathode assembly and the gun cell (1st cell of a 9 cell accelerator structure) is not only novel and a key part of the full system; it is critical for achieving stable intensity and high-average power.

In our concept, we chose to use a 9-cell standard 'accelerating' structure that was originally developed for the TeV–Energy Superconducting Linear Accelerator (TESLA) which is a superconducting electron–positron collider of initially 500 GeV total energy, extendable to 800 GeV, and an integrated X–ray laser laboratory at DESY, Germany [6]. This structure is also called ILC/XFEL cavity since it uses in International Linear Collider and European X-Ray Free Electron Laser machines [7,8]. In their cases, there is an electron gun that is a separate component, and therefore not a fully integrated design. The ILC/XFEL accelerating structure utilizes an elliptical RF cavity profile that is fabricated with high-purity niobium and operates at 2 K. This structure is designed to run at a resonant RF frequency of 1.3 GHz and represented a good starting point for our design.

2. DETAILED ELECTROMAGNETIC SIMULATIONS OF THE INTEGRATED STRUCTURE

In an electron source, the cathode system is critical for achieving stable intensity and high-average power. The envisioned gun will provide short bunches injected into a specified phase range of the RF cycle. Done correctly this will limit the current intercepted by the superconducting walls and will prevent an unwanted load on the cyro-cooler system.

In our design, we have integrated gun cavity into the first cell of a standard, 9-cell, 1.3-GHz ILC/XFEL (International Linear Collider/European X-Ray Free Electron Laser) cavity to form an 8.4-cell 'electron source'. The latter eight cells are for acceleration and the first modified cell (with a length ratio of 0.4 of a full cell) contains the cathode system and provides the initial acceleration. This design feature is key to the overall compact design, i.e. it is fully integrated. The length of the first cell is primarily chosen to account for the difference between the average velocity of the electrons in the cell compared to the phase velocity, *c*. We have used several simulation codes to design this unique system and validate our architecture.

2.1. Design of the Gun Cell and Overall Accelerating Structure

In our accelerator design, the 8 cells of the standard ILC/XFEL cavity parameters are used and the 1st cell of this structure is redesigned to match the desired parameters of an integrated electron gun. For this step, the first cell of the 9-cell is modified using SUPERFISH [9], so that it would be suitable for the initial cell containing the cathode

region. To begin, a 9-cell ILC/XFEL superconducting elliptical cavity geometry file was created as a SUPERFISH geometry file using an internal code and transferred to SUPERFISH to ensure SUPERFISH would work correctly for future optimization and design studies. The details of the validation and 9-cell structure design results can be found in [10].

Then, the design optimization for the first (gun) cell of the desired configuration was started with the goal of obtaining the desired field distribution in the π-mode (adjacent cells operating 180 degrees out of phase with one another) and at the chosen 1.3-GHz frequency. To meet these requirements, we have optimized the design parameters which are given in Table 1.
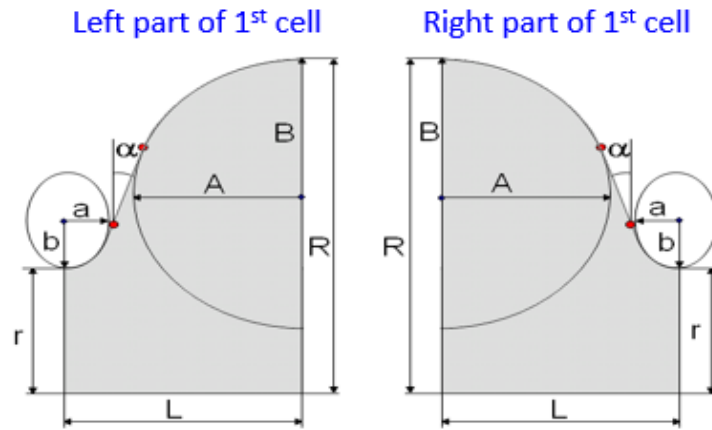
Figure 2: The parameters of an elliptical cavity's design geometry. The parameter values of the modified (gun) cell are given in Table 1.

The initial design parameters were calculated for the geometry of an elliptical cavity as shown in Figure 2. Tolerances are assumed to be ± 100 μm during this RF design optimization. These values will be recalculated for the fabrication process, taking into account the dimensions of a cooled cavity and the chemical treatment of cavity surfaces.

Table 1. The design parameters of the modified (gun) cell

Design Parameters	Left part [mm]	Right part [mm]
Iris Radius, r	3.5	35
Cavity Radius, R	99.05	99.05
Length, L	12.93	34.59
External Radius, A	11.53	24
External Radius B	11.53	24
Horizontal Half Axis, a	1.4	9.2
Vertical Half Axis, b	1.4	12
Wall Slope, α	0°	2.6 °

A frequency scan of the 8.4-cell structure [10] performed with the code SUPERFISH and one frequency which is 1300.92 MHz gave the desired TM_{01} mode. This is the pi-mode frequency of the standard ILC/XFEL geometry design.

Figure 3 shows the 8.4-cell structure and field map with arrows and contours. Figure 4 is the magnified view of Figure 3 for the first 2 cells to illustrate the field map of the 8.4-cell cavity's geometry.

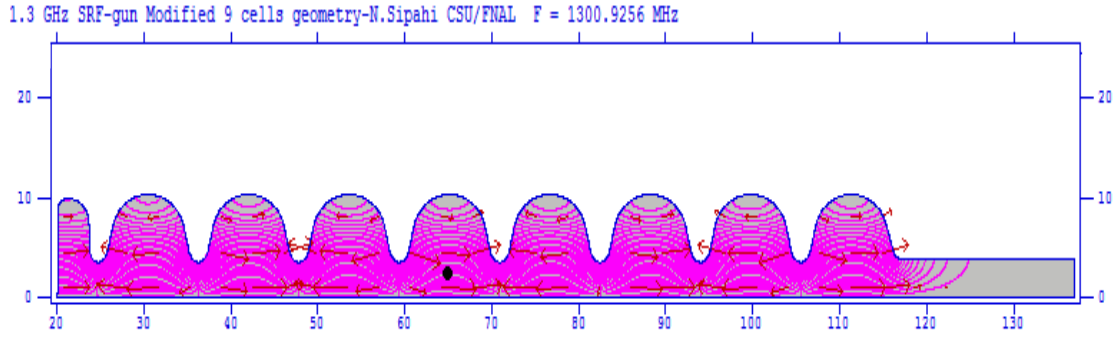Figure 3: The 8.4-cell structure's design geometry matched to the 1.3-GHz frequency and its field map in SUPERFISH.
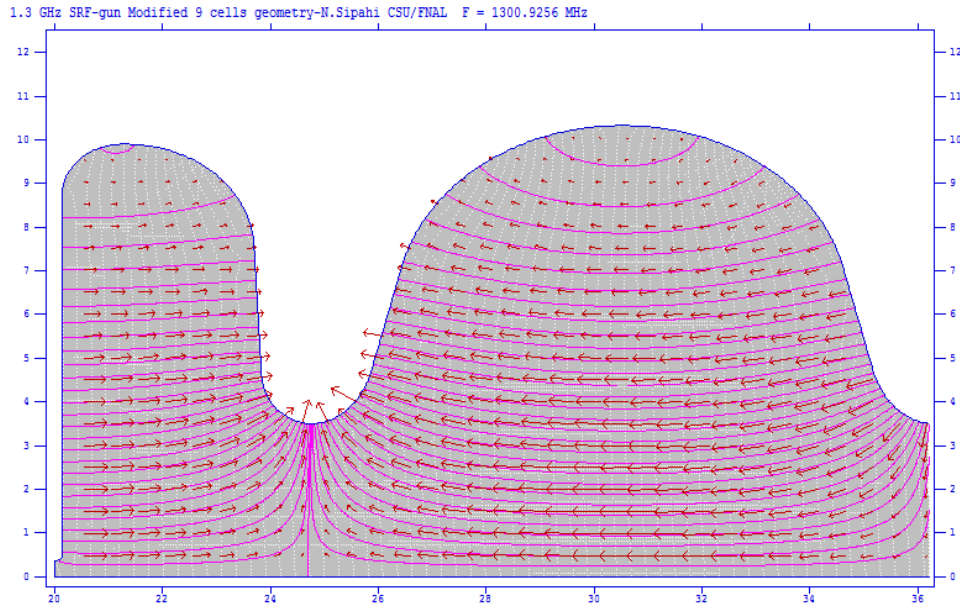

Figure 4: The magnified view of the first 2 cells shown in Figure 3.

Figure 5 shows the on-axis field distribution of the 8.4-cell accelerating cavity. The field in the first "cell" has been optimized based on the design conditions to achieve maximum gradient in the first cell cavity.
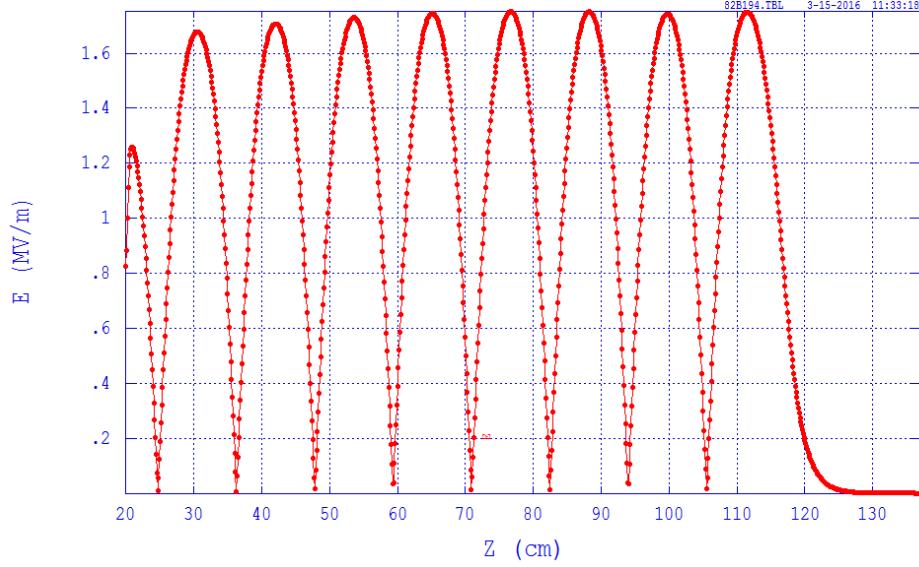
Figure 5: The electromagnetic field distribution of our 8.4-cell structure's design geometry as computed by SUPERFISH.

Moreover, two additional simulations tools were used as a check on the results: the 2-D code COMSOL Multiphysics [11] and the full 3-D code CST MWS [12] and the results are given in Appendix A [13]. Strong agreement was found in all three cases. We will present in the primary text only the SUPERFISH results since these results have been used as the input for the beam dynamics simulation part [15].

As a next step, the design steps were repeated for the case of a shorter first cell – a length of 0.3 of a full cell. This allowed us to perform some design optimization of the gun cell length based on the metrics of the beam's performance will be performed in later. As can be seen in Table 2, the output parameters are quite similar to those found with a first cell length of 0.4 of a full cell.

Table 2: The results of SUPERFISH for two different lengths of the first cell (0.3 and 0.4 of a full-cell length)

Parameters	SUPERFISH	
Gun Cell Ratio	0.4	0.3
Frequency [MHz]	1300.9	1300.9
E_{peak}, [MV/m]	21.7	22.6
B_{peak}, [mT]	45.1	45.4
B_{peak}/E_{peak} [mT/(MV/m)]	2.07	2.0
R/Q [Ω]	931	908

2.2. Design of the Cathode Region

We have chosen a thermionic cathode for our design. Since a thermionic cathode is by its very nature operated at high temperature, this could present an issue within a superconducting environment; however, it is not as problematical as it can be imagined.

The cathode will be operated in vacuum and we will assume that a very low thermal conductivity holder holds it in place. Power (heat) radiated from the cathode into the RF cavity structure region is then dominated by black-body radiation. According to Stefan-Boltzmann equation, operation at even slightly lower temperatures will drop this number dramatically and increase the cathode lifetime, but at the expense of a lower current density (the details can be found in [10]).

The cathode region is designed with a 70 K shield just downstream of the cathode. The aperture of this shield is such that it intercepts any heat that would otherwise directly impact the superconducting surfaces. Because the RF cavity apertures are very large

they are effectively in the shadow of this shield plate and so do not directly see the cathode therefore limiting the impact of the heat from the cathode on the superconducting surfaces.
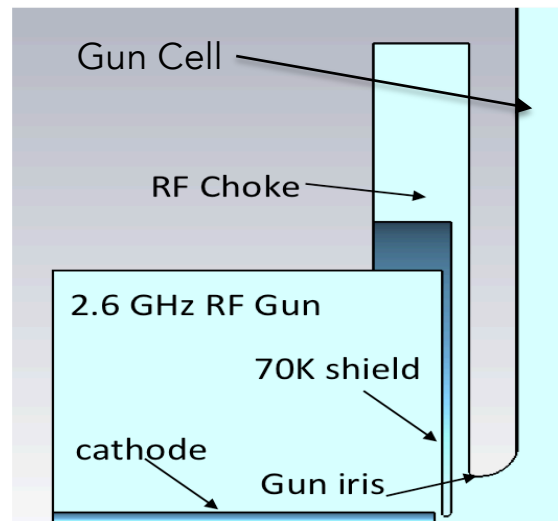

Figure 6: Schematic view of the cathode assembly indicating 70K shielding and RF choke

We also make the assumption that a suitable thermionic cathode material can be found that will, in itself, not contaminate the superconducting environment. The first choice is the M-type dispenser cathode as these have proven quite robust and have sufficient emission at relatively low temperature. We are also considering other cathodes, including field emitters for a future step, should the thermionic cathode design prove intractable.

One significant issue with a thermionic cathode system is that it will emit electrons if the RF field at the cathode is the correct sign. If the cathode is subjected to only the fundamental 1.3-GHz field then it will emit electrons over a full 180 degrees. Unfortunately, not all these electrons will make it out of the accelerator. Many will either

strike the superconducting surfaces and present a significant heat source or back bombard the cathode. Therefore electron emission must be gated to limit phase range of emission that will ensure acceleration of the electrons without them striking the superconducting surfaces or back bombarding the cathode. This gating process is illustrated in Figure 7.
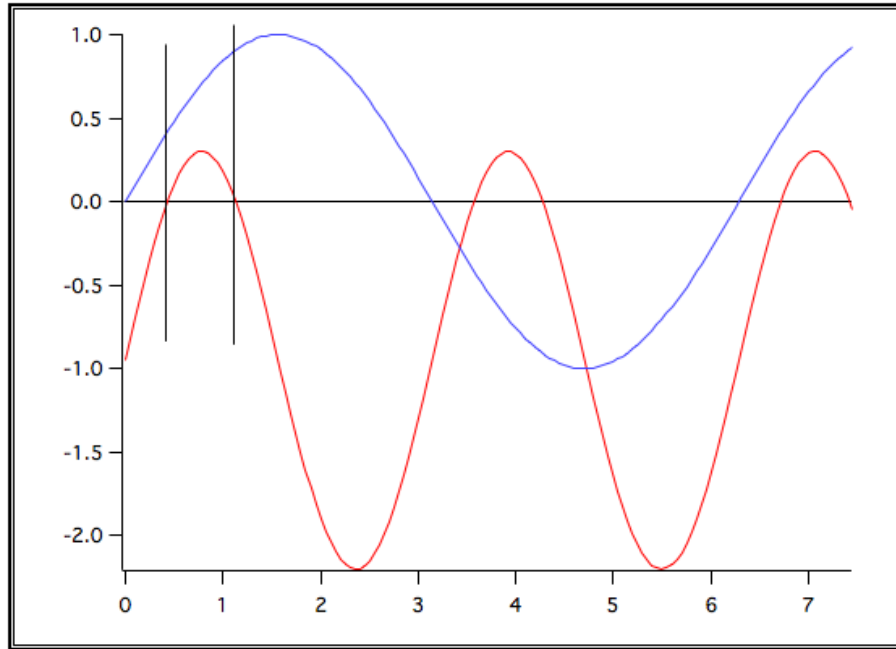

Figure 7: The gating process using fundamental frequency (1.3 GHz) and second harmonic of the fundamental frequency (2.6 GHz). The blue line indicates the fundamental frequency and red line indicates the second harmonic.

To implement the gating of charge from the cathode surface, we have incorporated an additional resonant cavity behind the cathode plane of the half-cell that is designed to be resonant at the second harmonic of the main frequency, i.e. at 2.6 GHz; this region will also be held at a DC bias. From Figures 8 through Figure 14 show this region both separately and coupled to the 8.4-cell accelerating structure. By judicious choice of the fundamental and second harmonic field amplitudes, the relative phases between the

two RF fields, the DC bias field and the carefully chosen longitudinal location of the cathode we are able to effectively and simply gate the electrons over the desired range of RF phases.

The detailed design of this region was done in several steps. First, the cathode 2.6 GHz resonant region was separately designed [25]. Again, we used SUPERFISH to examine the geometry and the fields. The results from COMSOL and CST MWS are also shown in the Appendix B. During the design process, the two important parameters are the length of the 70K shielding and the location of the RF choke in order to resonant the cathode assembly at 2.6 GHz. After the several optimization steps [10] the geometry has been optimized. Figure 8 shows the optimized cathode geometry (which is operating at 2.6 GHz frequency).
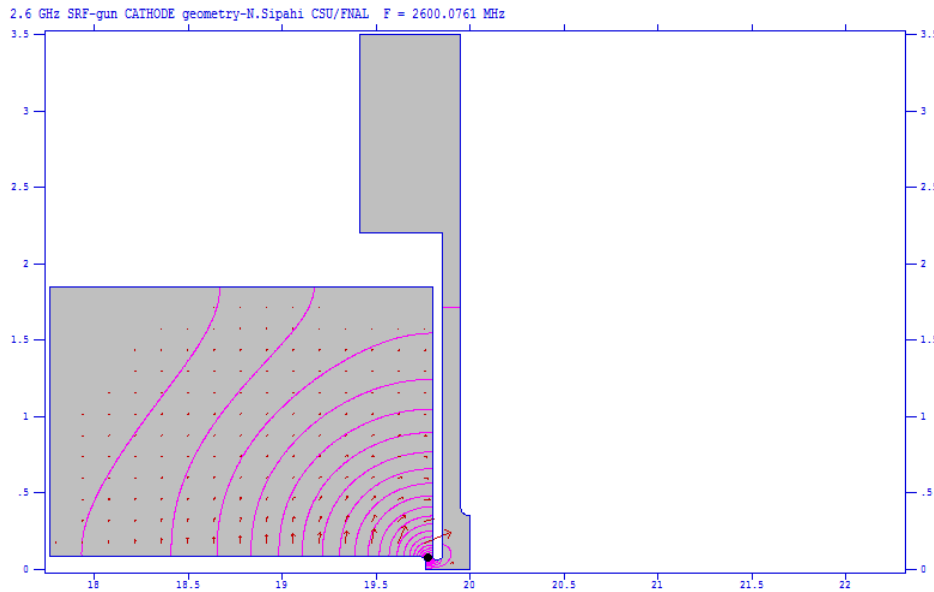

Figure 8: The cathode region's design geometry at 2.6 GHz with the field generated using SUPERFISH.

2.3. Design Combination of the Cathode and the Gun into a Single Structure

Until here, the results shows how we separately designed the cathode and accelerator regions of the entire desired structure. We now show the design results of combined structure [14].

Using SUPERFISH, we first checked the impact on the resonance conditions when we combined the two structures into one. As can be seen in Figure 9, the field from the 8.4-cell structure when excited solely at the fundamental frequency of 1.3 GHz does not propagate through the iris to the cathode region.
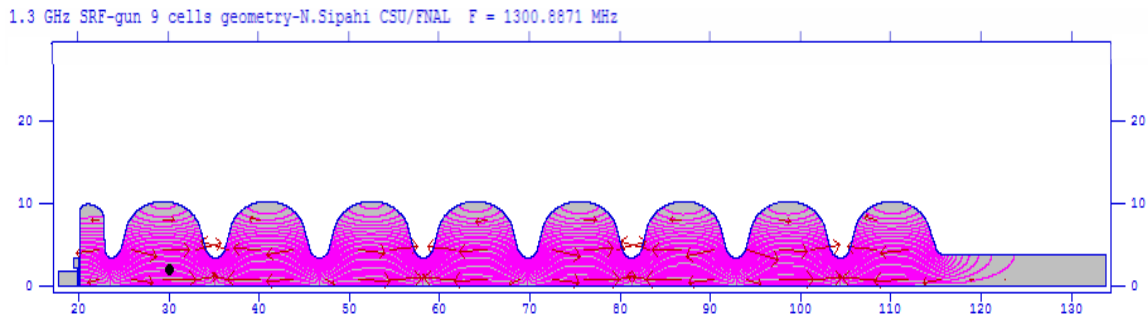

Figure 9: The design geometry of the combined cathode and gun regions at 1.3 GHz as calculated using SUPERFISH.
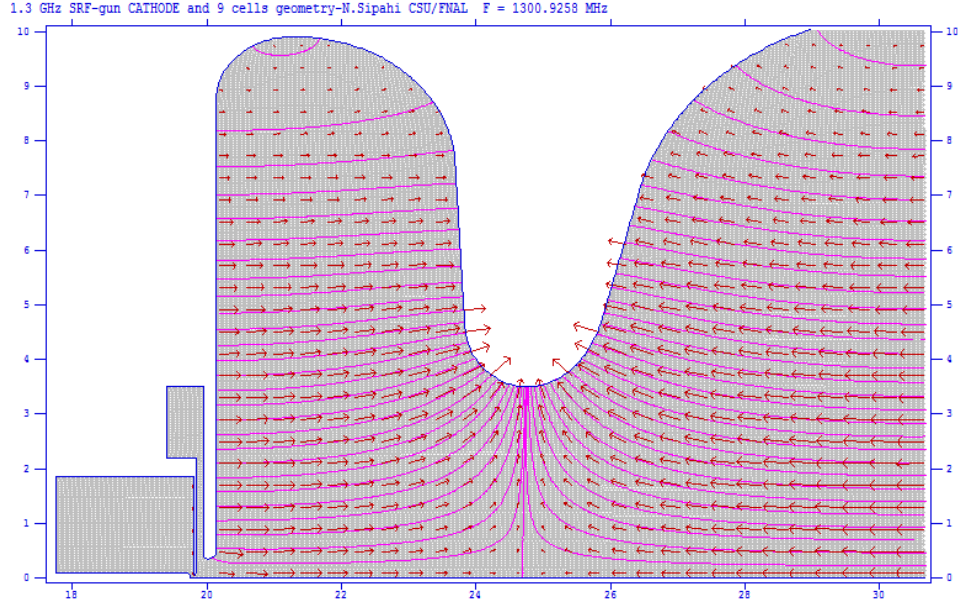
Figure 10: The magnified view of the cathode and the first cell regions when integrated as shown in Figure 9 as calculated using SUPERFISH.

Similarly, if we excite only the cathode region at 2.6 GHz it can be seen that there is very little coupling of field into the main accelerating region (Fig. 11) and will be completely inconsequential compared to the dominant 1.3-GHz frequency component. In affect the two regions are independent.
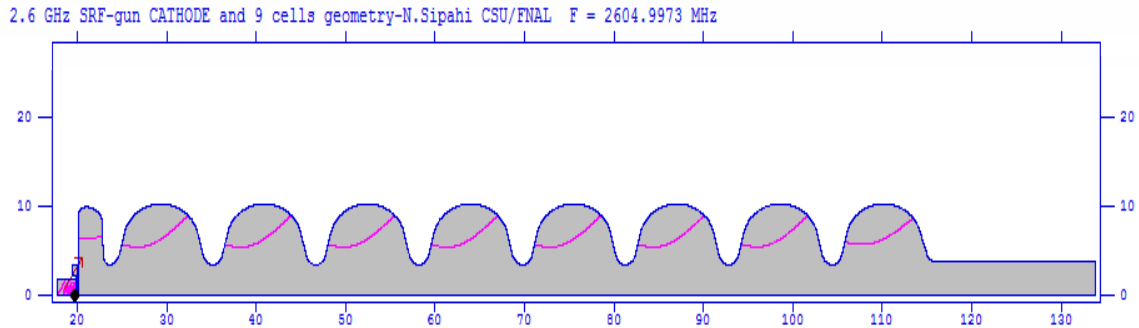

Figure 11: The design geometry of the cathode and gun structures together and the results at 2.6 GHz.
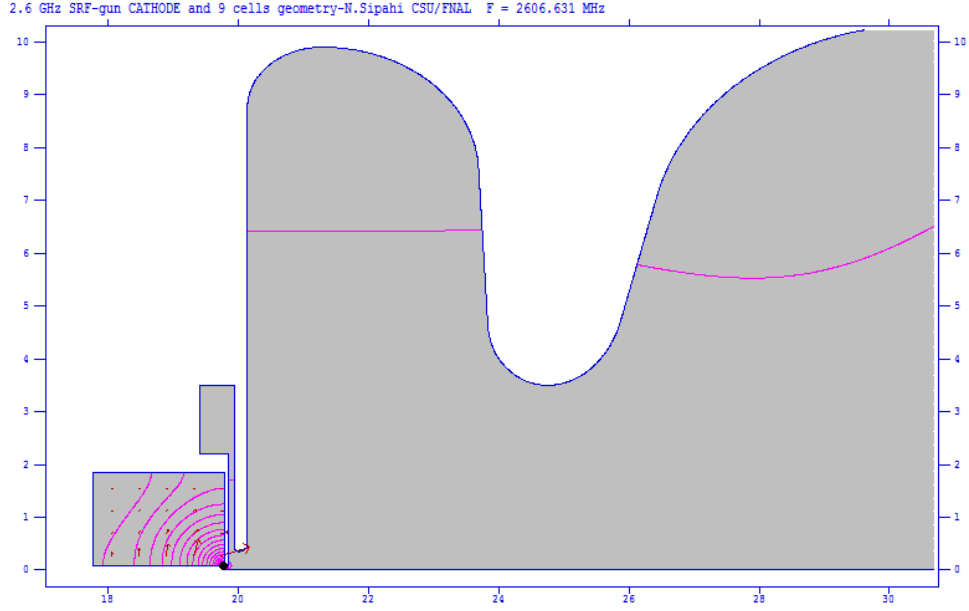
Figure 12: The magnified view of the cathode and first cell regions when integrated as shown in Figure 11 as calculated using SUPERFISH.

3. SUMMARY

As a summary of this report, we have performed simulations to design a compact 1.3 GHz accelerating structure with an integrated cathode based on a 9-cell ILC/TESLA SCRF structure. We designed the cathode region for a gun geometry where the 8.3-cell region is resonant at 1.3 GHz and the cathode region is resonant at 2.6 GHz. This design, together with a DC bias field will allow gating of the electrons into the main

structure over a range of RF phases favorable to acceleration without loss of beam on the SC surfaces or through back-bombardment. We have used the SUPERFISH (also COMSOL Multiphysics codes and the 3D CST MWS) during design process. The detailed beam dynamics studies of this integrated system are presented in another technical report [15].

Acknowledgement

References

[1] A. Grassellino, A. Romanenko, D. Sergatskov, O. Melnychuk, Y. Trenikhina, A. Crawford, A. Rowe, M. Wong, T. Khabiboulline and F. Barkov, "Nitrogen and argon doping of niobium for superconducting radio frequency cavities: a path way to highly efficient accelerating structures", Supercond. Sci. Technol. 26, 102001 (2013).

[2] B. Chase, R. Pasquinelli, E. Cullerton, P. Varghese, "Precision Vector Control of a Superconducting RF Cavity driven by an Injection Locked Magnetron", Patent pending.

[3] Kazakevich, Grigory, and Rolland Johnson. "High-power magnetron RF source for superconducting Linacs of ADS and intensity-frontier projects."*Presented at 11th International Topical meeting on Nuclear Applications of Accelerators*. No. FERMILAB-CONF-13-314-AD-TD. 2013.

[4] S. Kazakov, "How to Eliminate a Copper Coating and to Increase an Average Power of Main Coupler", TUPO009, Proceedings of SRF 2011, Chicago IL.

[5] R. Kephart, N.Sipahi, et al., "SRF and Compact Accelerators for Industry and Society", IPAC2015, Richmond, 2015.

[6] Richard, F., et al. "TESLA Technical Design Report Part I: Executive Summary." *arXiv preprint hep-ph/0106314* (2001).

[7] Phinney, Nan, Nobukasu Toge, and Nicholas Walker. "ILC reference design report." *arXiv preprint arXiv:0712.2361* (2007).

[8] Altarelli, Massimo, et al. "The technical design report of the European XFEL."*Chapter* 4 (2006): 2006-097.

[9] K. Halbach and R.F. Holsinger, SUPERFISH - A Computer Program for Evaluation of RF Cavities with Cylindrical Symmetry, Part. Accel., 7 (1976) 213 - 222.

[10] Sipahi, Nihan. "Design Of An Integrated Compact High Power Superconducting Radio Frequency Electron Beam Source and Klsytron-Inspired Compact and Tunable THz Power Source" PhD diss, Colorado State University, will be published.

[11] COMSOL Multiphysics Manual 5.1, see https://www.comsol.com/comsol-multiphysics

[12] CST Microwave Studio: https://www.cst.com/products/CSTMWS

[13] Sipahi, Nihan, et al. "RF Design of a High Average Beam-Power SRF Electron Source." *7th International Particle Accelerator Conference (IPAC'16), Busan, Korea, May 8-13, 2016*. JACOW, Geneva, Switzerland, 2016.

[14] Sipahi, Nihan, et al. "RF Design of a 1.3-GHz High Average Beam Power SRF Electron Source." *North American Particle Accelerator Conf.(NAPAC'16), Chicago, IL, USA, October 9-14, 2016*. JACOW, Geneva, Switzerland, 2017.

[15] Sipahi, N., "Part 2: Initial Beam Dynamics Results of an Integrated and Compact 1.3 GHz Superconducting Radio Frequency (SRF) Electron Source, Fermilab National Laboratory, Batavia, IL (in press).

APPENDIX

A. Additional Design Results for the Gun-cell and Overall Accelerating Structure

In this part, the detailed simulation results in Comsol Multiphysics and CST Microwave Studio have been presented.

Figures 13 and 14 show the simulation results of the 8.4-cell cavity design via COMSOL Multiphysics. As we expected, the results match with the SUPERFISH results shown in Figure 3 and 5, respectively.
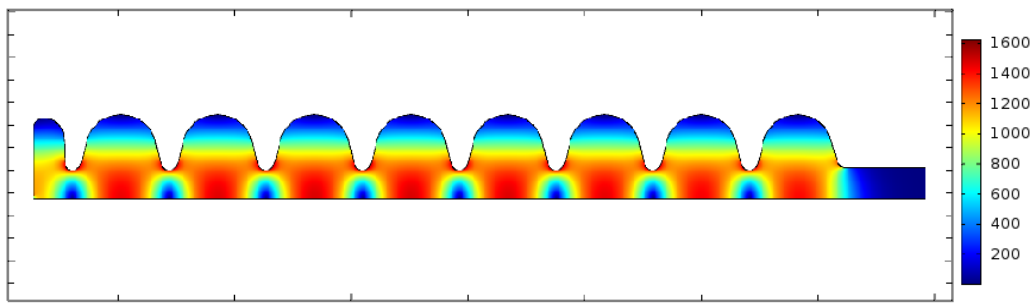

Figure 13: The 8.4-cell structure's design geometry with the frequency matched to 1.3 GHz and its field map as generated in COMSOL Multiphysics.
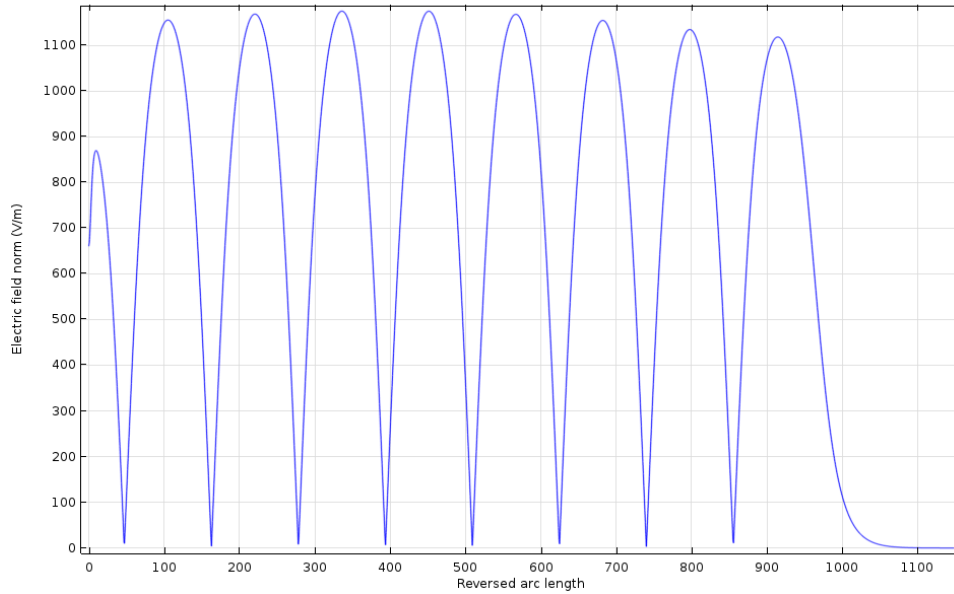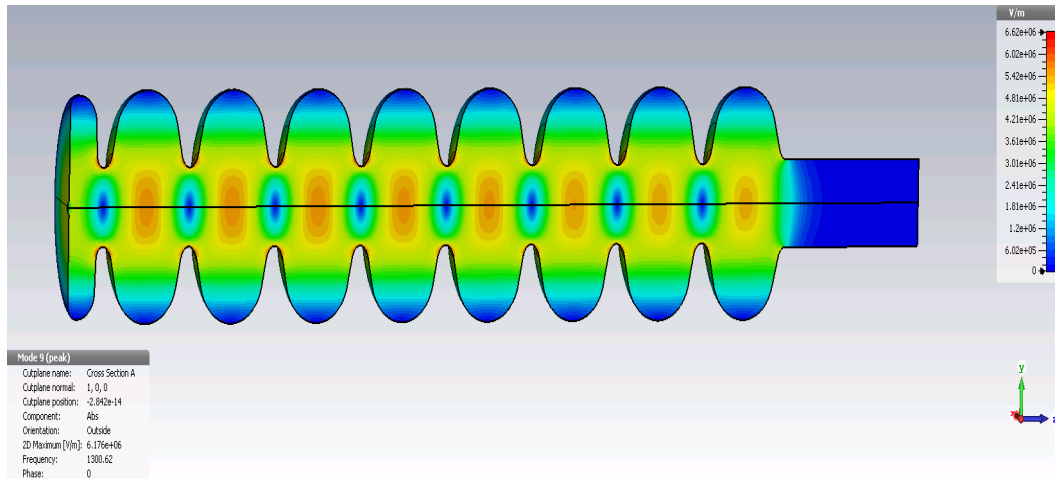
Figure 14: The electromagnetic field distribution of the 8.4-cell structure's design geometry as generated in COMSOL Multiphysics.

Moreover, Figures 15 a, b and 16 show the CST MWS simulation results for 8.4-cell structure and they are also in good agreement with the results of the 2-D simulations obtained from both the SUPERFISH and COMSOL Multiphysics codes.
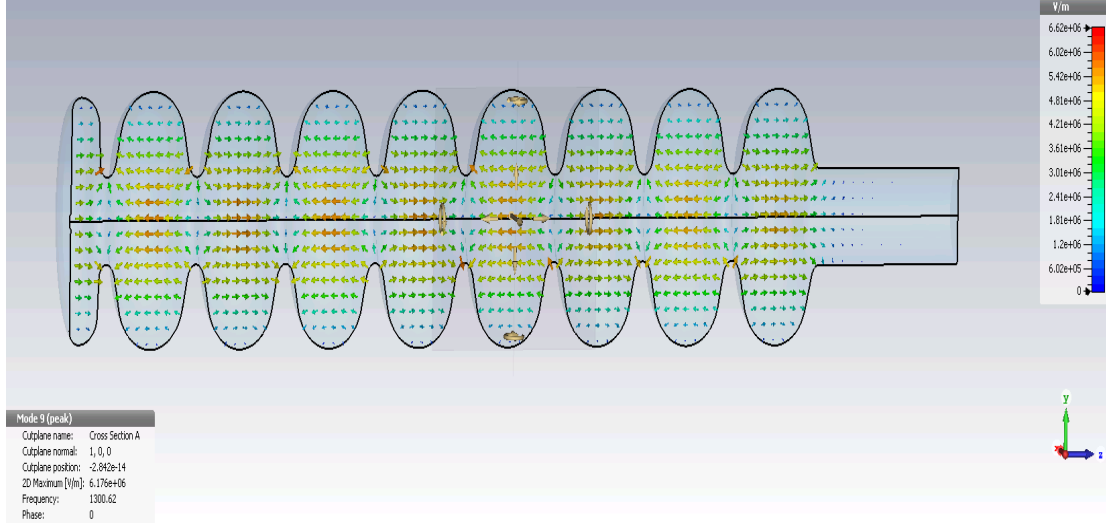
Figure 15: The 8.4-cell structure's design geometry with the frequency matched to 1.3 GHz and the contour plot of the fields using CST MWS b) The 8.4-cell structure's design geometry with the view of the fields in the pi mode using CST MWS.
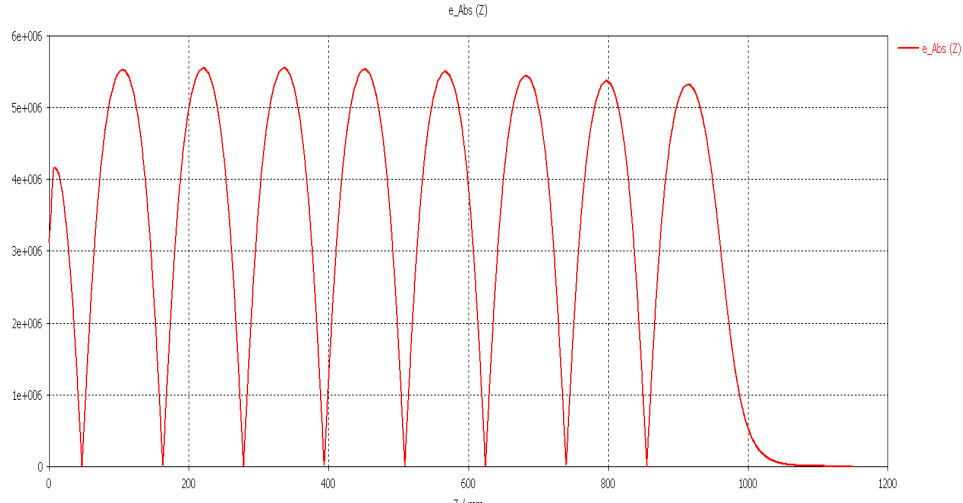

Figure 16: The electromagnetic field distribution of the 8.4-cell accelerating section's design geometry as determined with CST MWS.

In Table 3, we summarize and compare the results obtained from the three different simulation codes for these two different first cell lengths. While the normalization between the various codes is different, the resonant frequencies of the TM_{01} modes are quite similar as generated by SUPERFISH, COMSOL and CST. Differences can be attributed to the different meshing techniques used in the various codes; however, the

values obtained are suitable for these particular RF design optimizations. Finally, as seen in Table 3, the values of the field profiles are lower in the 0.3 cell case than in the 0.4 length cell case. Initial beam dynamics simulations show better overall performance in the 0.3 cell case, particularly in the area of beam loss; therefore, we have chosen to pursue this case in more detail.

Table 3: The results of SUPERFISH, COMSOL Multiphysics and CST MWS for two different lengths of the first cell (0.3 and 0.4 of a full-cell length). The peak fields are calculated for 10-MeV output electron beam energy.

Parameters	SUPERFISH		COMSOL Multiphysics		CST MWS	
Gun Cell Ratio	0.4	0.3	0.4	0.3	0.4	0.3
Frequency [MHz]	1300.9	1300.9	1299.9	1300.7	1300.6	1300.6
E_{peak}, [MV/m]	21.7	22.6	22.5	24.3	22.5	23.8
B_{peak}, [mT]	45.1	45.4	44.4	45.5	44.6	44.7
B_{peak}/E_{peak} [mT/(MV/m)]	2.07	2.0	1.97	1.87	1.98	1.88
R/Q [Ω]	931	908	942	910	936	908

B. Additional Design Results for the Cathode Assembly

This part represents the COMSOL Multiphysics design results and shows the validation with our SUPERFISH results. The result using COMSOL Multiphysics is given in Figure 17, illustrating the cathode geometry and field distribution. As it was seen in the design process of the 8.4-cell accelerating structure, the design results using the 2-D codes, SUPERFISH and COMSOL provide again comparable results also for the cathode region.
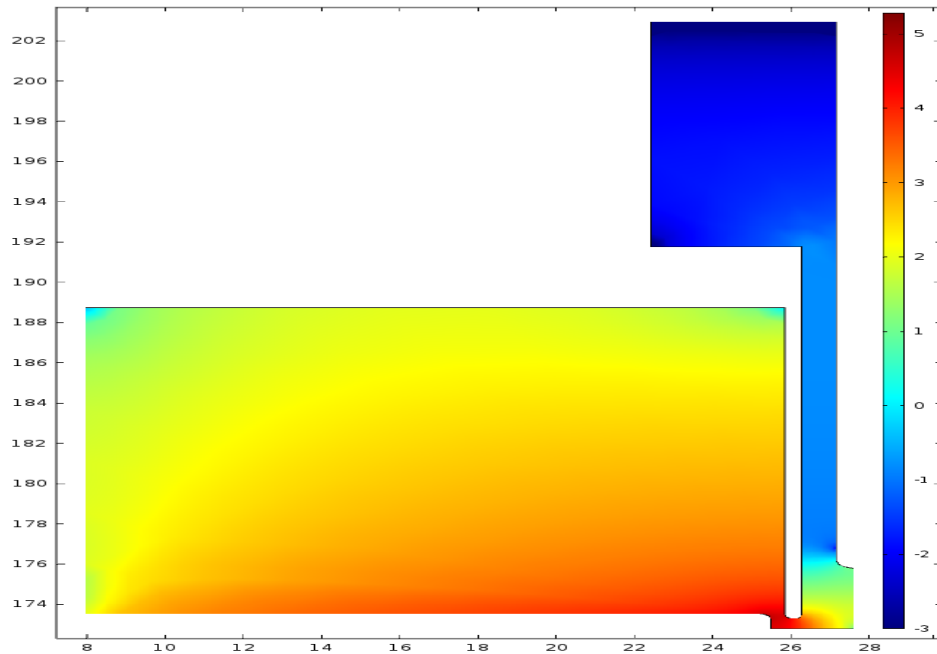

Figure 17: The cathode region's design geometry at 2.6 GHz and field map (in logarithmic scale) using COMSOL Multiphysics

We further validated the 2D results using CST MWS. This result is shown in Figure 18, and illustrate that CST provides analogous results as compared to SUPERFISH and COMSOL.
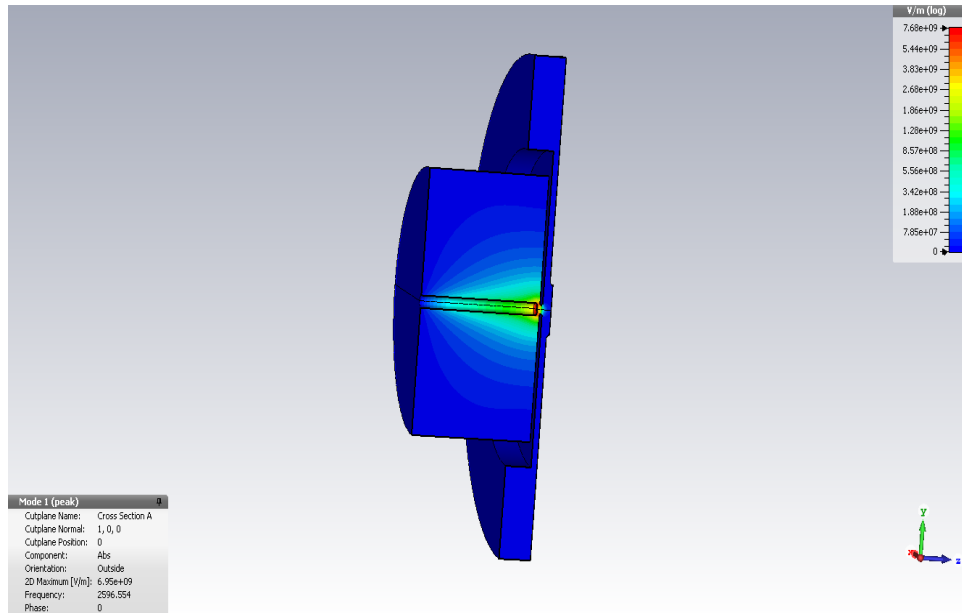
Figure 18: The cathode region's design geometry with the frequency matched to 2.6 GHz and the contour plot of the fields as generated in CST MWS.

C. Additional Design Results for the Integrated System

Next, using COMSOL Multiphysics, we find similar results to those found as in SUPERFISH, and shown in Figures 9 – 12). COMSOL also shows that the dominant frequency is 1.3 GHz in Figures 19, 20 and 21. For the simulations of the 2.6-GHz frequency component through the combined structure, there is only negligible propagation to and through the first cell, as can be seen in Figures 22 and 23. The detailed comparison shows good agreement using our previous methods of design validation.
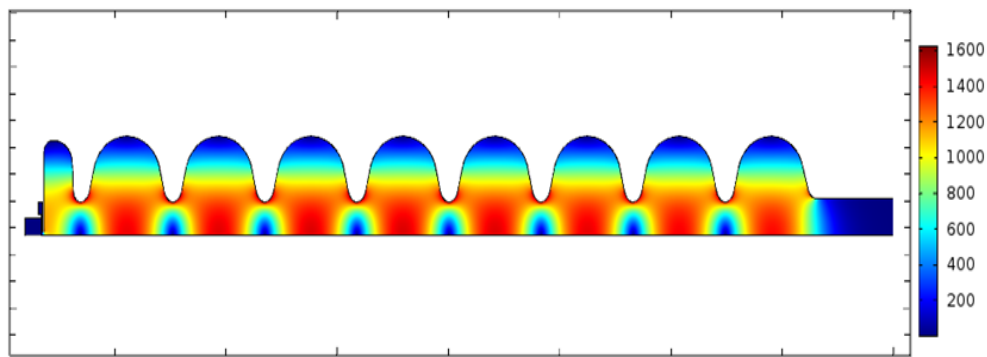

Figure 19: The geometry of the integrated cathode and accelerating structure at a frequency of 1.3 GHz as simulated with COMSOL Multiphysics.
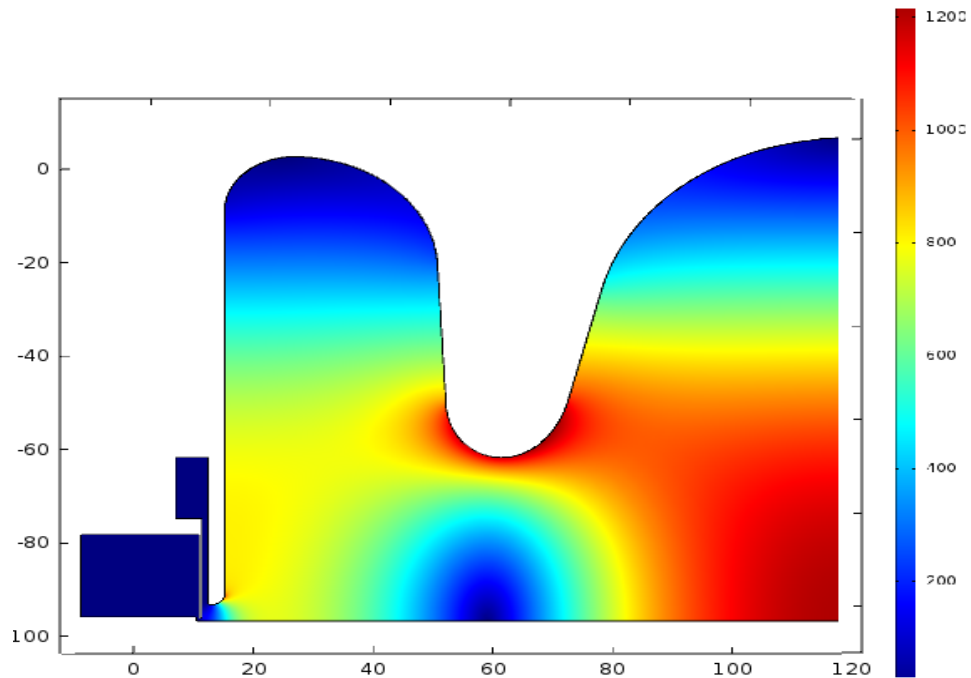
Figure 20: The magnified view of the cathode and first cell connection as shown in Figure 19 as calculated with COMSOL Multiphysics.
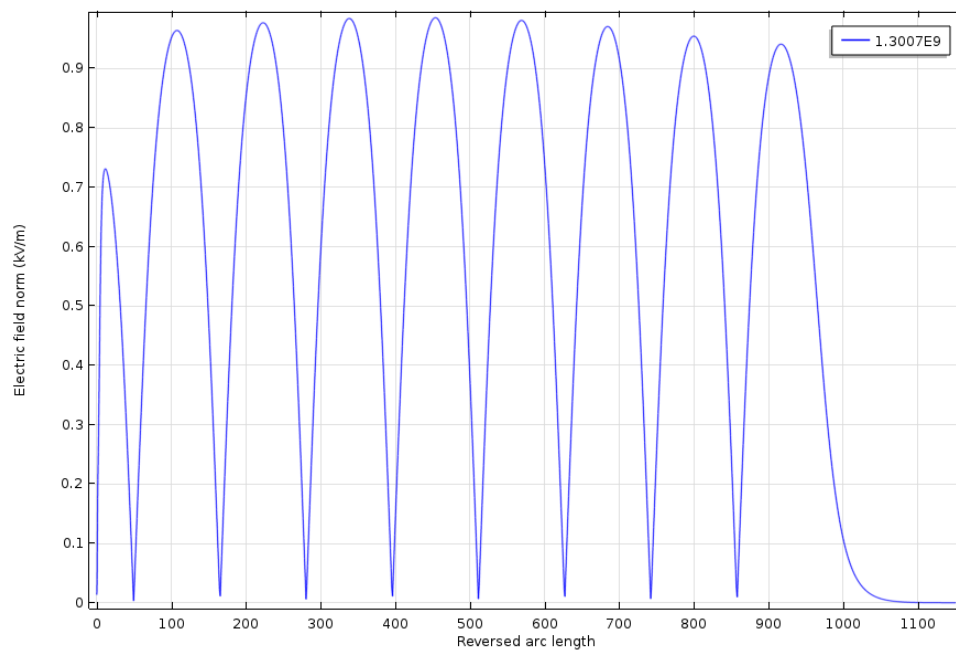

Figure 21: The field distribution for the design geometry given in Figure 19 using COMSOL Multiphysics.
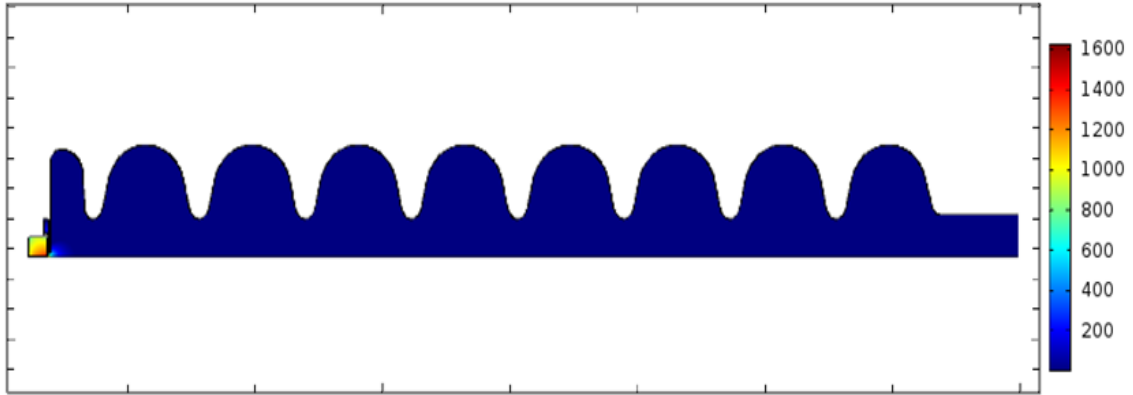
Figure 22: The geometry and frequency (at 2.6 GHz) of the integrated cathode and accelerating structure as simulated with COMSOL Multiphysics.
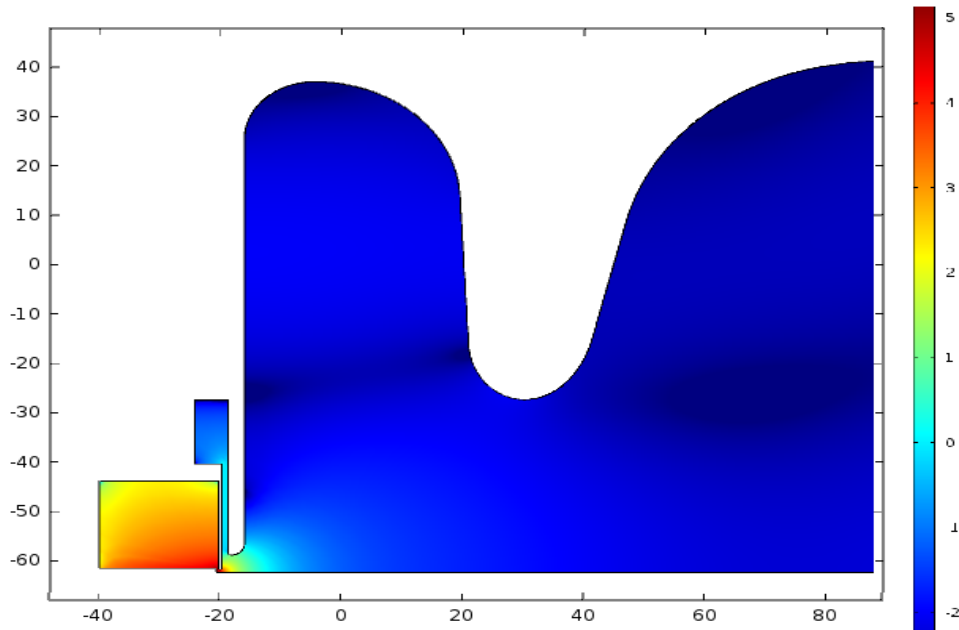

Figure 23: The magnified view of the integrated cathode and first cell as shown in Figure 22 in order to enhance the field map in the cathode region as calculated with COMSOL Multiphysics.